Internet of Things xxx (xxxx) xxx

Contents lists available at ScienceDirect

Internet of Things

journal homepage: www.elsevier.com/locate/iot

A novel medical image fusion method based on Rolling Guidance Filtering

Jingyue Chen[a], Lei Zhang[b], Lu Lu[a], Qilei Li[a], Moufa Hu[c], Xiaomin Yang[a,*]

[a] College of Electronics and Information Engineering, Sichuan University, Chengdu, Sichuan, 610064, China
[b] College of Computer science, Sichuan University, Chengdu, Sichuan, 610064, China
[c] National Key Laboratory of Automatic Target Recognition (ATR), National University of Defense Technology, Changsha, Hunan, 410073, China

ARTICLE INFO

Article history:
Received 1 July 2019
Revised 23 November 2019
Accepted 23 November 2019
Available online xxx

Keywords:
Medical image fusion
Rolling Guidance Filtering
Structure-detail decomposition
Laplacian pyramid
Sum-modified-laplacian

ABSTRACT

Medical image fusion realizes the complementary advantages of information between different modality medical images to obtain more comprehensive and precise image results. In order to better preserve valid structural information and detail textures of source images, we propose a novel medical image fusion method in this paper. Firstly, we adopt a Rolling Guidance Filter to separate source medical images into structural component and detail component. The Laplacian Pyramid based fusion rule is used to merge the structural component. For the detail component, a sum-modified-laplacian (SML) based method is employed. At last, the result is acquired by integrating the fused structural and detail components. Experimental results demonstrate that the method is superior to conventional medical image fusion methods.

1. Introduction

Medical images of different modality have their own advantages and limitations. For example, computed tomography (CT) is excellent to the combination imaging of bones, and blood vessels, while almost powerless to soft tissue. Magnetic resonance imaging (MRI) is the reverse, which sensitivity to soft tissue higher than CT whereas it is barely visible for bone tissue. Therefore, an appropriate integration for medical images of different modality becomes an urgent need in clinicians diagnose and treating diseases [1]. Generally, there are two techniques can be used to integrate different modality medical images. One technique is to upgrade hardware devices. This way is straightforward but complex and expensive. Another low-cost technique is image processing. That is a convenient way to obtain an integrated image. In recent years, numerous research efforts were made to ameliorate the medical image. Image fusion is an effective technique to amend human eye visibility, which can integrate the complementary advantages of information between different modality medical images. The existing image fusion methods can be roughly classified into spatial domain and transform domain based methods.

Spatial domain based methods extract interesting information directly to fuse images without decomposition and reconstruction. The classical spatial domain based methods include the weighted average fusion method [2], IHS color space transform fusion method [3], neural network-based fusion method [4], etc. This kind of methods has the advantages of low computational complexity, good real-time performance and high signal-to-noise ratio of fused images. However, it may lead to edge blur, lower contrast, and sharpness declined [5].

* Corresponding author.
E-mail address: arielyang@scu.edu.cn (X. Yang).

https://doi.org/10.1016/j.iot.2020.100172
2542-6605/

Please cite this article as: J. Chen, L. Zhang and L. Lu et al., A novel medical image fusion method based on Rolling Guidance Filtering, Internet of Things, https://doi.org/10.1016/j.iot.2020.100172

Generally, transform domain based method is more widely used, which applying transform tools decomposes an image into a transform base and coefficients. Afterwards, various fusion strategies are applied to merge coefficients to obtain the fused results. In 1983, Burt and Adelson [6] proposed the Laplace pyramid (LP) algorithm, which opened the prelude of multi-scale transform fusion methods. Toet [7] propose a contrast pyramid transform method. This method can retain more details than the Laplacian pyramid algorithm. In recent decades, many improved versions of transform domain based methods have been proposed. A wavelet transform based methods is proposed in [8]. Discrete wavelet transform (DWT) [9] is an improved version of the wavelet transform method. In [10] propose a dual-tree complex WT (DTCWT) for improving the issue of detail lost. Non-subsampled contourlet transform (NSCT) [11] solves the troubles of direction restriction and translation invariance in wavelet transform (WT) and DWT. On the basis of the LP algorithm, Du jiao et al. [12] applied the multi-character Laplace pyramid in the medical image fusion method and proved its feasibility. The composite images obtained by these methods have rich information and fast fusion speed. Thence, there are still many scholars at home and abroad to study the medical image fusion algorithm based on pyramid decomposition.

To make better use of image geometry information for improving the quality of fused images, multi-scale decomposition theory comes into being. The Ridgelet transform and Curvelet transform, are representative multi-scale decomposition methods, are proposed in [13,14], respectively. Non-linear edge-preserving filtering has been introduced to construct multi-scale representations of image fusion of late years. [15] presents a fast and effective method for image fusion with guided filtering (GF). Gan et al. [16] applied weighted least squares filtering (WLS) to image fusion, which can obtain a better result than the previous multi-scale based method. However, this method is hard to expedite the fusion procedure. Wei Jiang et al. in [17] perform the WLS and LP-SR based method for image fusion. This method improves fusion speed and fusion quality. In 2014, Qi Zhang et al. [18] propose a novel edge-preserving filtering, that is Rolling Guidance Filtering (RGF). It can achieve fast convergence in view of its rolling guidance based on iterative implementation. In [19,20], L et al. and Jian et al. use RGF to implement multi-modality image fusion, respectively. The results evince that RGF can which can effectively eliminate artifacts and is superior to other edge-preserving filters in some extent.

Sparse Representation (SR) was derived from compressed sensing [21–23]. In recent years, SR has attracted much attention with its excellent adaptability and flexibility, and many application examples can be found in different fields [24,25]. Yang and Li in [26] adopt SR to image fusion firstly, as a transform domain method. In [27], Li et al. utilize the guided filtering and dictionary learning to achieve image fusion. In [28], Zhu et al. propose an image fusion method based on dictionary learning with KSVD, which can effectively represent the details of an image. Targeted flexible models, computational speed, adaptive, and high-performance representations are key issues for sparse representation methods to leverage their strengths in the application domain.

In this paper, we present a medical image fusion method based on Rolling Guidance Filtering. The method can not only remain clear edge information but also maintain the energy of the source image. First, we decompose the source images to the structural component and the detail component by utilizing the Rolling Guidance Filter. The RGF can preserve the edge information automatically to achieve large-scale structure optimization. Second, diverse strategies are come up to deal with the structural and detail components. For structural component, an LP-SR based fusion rule is employed to retain the structural and spectral information. For the detail component, we utilize the Sum-Modified-Laplacian (SML) for preserving the energy of source images. Finally, the fused result is synthesized with the processed structural and detail components.

The contributions of this paper can be described briefly as following:

1.) The method utilizes the Rolling Guidance Filter to decompose source image into the structural component and the detail component. The RGF can ensure the accuracy of large-area object boundaries as well as remove and smooth complex small areas in an image.
2.) LP-based fusion rule is exploited to merge the structural component for preserving structural and spectral information. Fusion is performed separately on each spatial frequency layer. Therefore, different fusion operators can be used for highlighting features and details on specific frequency bands for features and details on different frequency bands of different decomposition layers.
3.) For the detail component, we utilize the Sum-Modified-Laplacian for remaining the energy of source image. SML can reflect the edge feature information and have excellent power of clarity discrimination of an image in some extent.

In the subsequent sections, we carry out a detailed introduction of the proposed method. We briefly review the RGF, LP, and SML in section 2. The detailed step of the method is exhibited in section 3. Experimental results and analysis are shown in section 4; The last section summarizes the paper.

2. Related work

2.1. Rolling Guidance Filtering

Zhang et al. [18] present a Rolling Guidance Filtering algorithm, is an edge-preserving smoothing filtering. The RGF implements rolling guidance based on an iterative manner, which has the characteristics of rapid convergence. Unlike other edge-preserving filtering, RGF can completely control the detail smoothing under the scale measure. RGF consists of two main procedures: small structure removal, edge recovery.

Please cite this article as: J. Chen, L. Zhang and L. Lu et al., A novel medical image fusion method based on Rolling Guidance Filtering, Internet of Things, https://doi.org/10.1016/j.iot.2020.100172

For the first procedure, we apply gaussian filtering to determine structure scale. We suppose that I and G indicate input and output images, respectively. x and y denote coordinates for an image. ς_d indicates standard deviation. The filter can be expressed as

$$G(x) = \frac{1}{K_x} \sum_{y \in N(x)} e^{\left(-\frac{\|x-y\|^2}{2\varsigma_d^2}\right)} \cdot I(y), \tag{1}$$

$$K_x = \sum_{y \in N(x)} e^{\left(-\frac{\|x-y\|^2}{2\varsigma_d^2}\right)},$$

$N(x)$ expresses the set of neighboring pixels of x.

For the edge recovery, we update an image J iteratively. Suppose J^{t+1} is represented as a result of the t-th iteration. Initially, J^1 represents the output value $G(x)$ in Eq. 1. σ_s and σ_r denote the spatial weight and range weight, separately. When the value of previous iteration J^t and the input I are given, the J^{t+1} can be calculated as

$$J^{t+1}(x) = \frac{1}{K_x} \sum_{y \in N(x)} e^{\left(-\frac{\|x-y\|^2}{2\sigma_s^2} - \frac{\|J^t(x)-J^t(y)\|^2}{2\sigma_r^2}\right)} \cdot I(y), \tag{2}$$

$$K_x = \sum_{y \in N(x)} e^{\left(-\frac{\|x-y\|^2}{2\sigma_s^2} - \frac{\|J^t(x)-J^t(y)\|^2}{2\sigma_r^2}\right)}.$$

In the framework of RGF, J^t is set as a constant C (*i.e.*, $\forall x$, $J^t(x) = C$), then we can simplify Eq. 2 to

$$J^{t+1}(x) = \frac{1}{K_x} \sum_{y \in N(x)} e^{\left(-\frac{\|x-y\|^2}{2\sigma_s^2}\right)} \cdot I(y). \tag{3}$$

Therefore, starting rolling guidance from J^0 can combine the two steps into one as $\forall x$, $J^0(x) = C$.

2.2. Laplacian pyramid

To describe the lost detail information of high-frequency by convolution and down-sampling operations in the process of Gaussian pyramid (GP), people define the Laplace pyramid (LP).

A series of difference images, as LP decomposition images, is obtained by subtracting the predicted image by each layer of GP after the operation of up-sampling and gaussian convolution for the previous layer. We set the low-resolution images as upper layers and high-resolution images as lower layers. The definition of the i-th Laplace pyramid as

$$L_i = G_i - U(G_{i+1}) \otimes g, \tag{4}$$

where G_i is the i-th image. $U(\cdot)$ represents up-sampling which mapping the (x, y) in an image to the target image $(2x + 1, 2y + 1)$. $\otimes$ indicates convolution. g is the Gaussian kernel, the size is 5×5.

2.3. Sum-Modified-Laplacian

Sum-Modified-Laplacian (SML) [29,30] can reflect the edge feature information as well as describe the sharpness of an image to some extent. Given an image I, the SML is described as

$$SML(x, y) = \sum_{m=-M}^{M} \sum_{n=-N}^{N} [ML(x + m, y + n)]^2, \tag{5}$$

$$ML(x, y) = |2 \cdot I(x, y) - I(x - s, y) - I(x + s, y)| + |2 \cdot I(x, y) - I(x, y - s) - I(x, y + s)|,$$

M and N determine the window size, that $(2M + 1) \times (2N + 1)$. s is the variable spacing. (x, y) is the spatial coordinate of image I.

3. The proposed method

We show the synopsis of proposed framework in Fig. 1. The method involves four main steps: image decomposition, structural component fusion, detail component fusion, and image reconstruction. We obtain structural component and detail component of source images by utilizing the Rolling Guidance Filtering in the first procedure. There are two different fusion strategies to deal with the structural and detail components, respectively. The fused structural and detail components reconstruct the final result in the step of image reconstruction.

Please cite this article as: J. Chen, L. Zhang and L. Lu et al., A novel medical image fusion method based on Rolling Guidance Filtering, Internet of Things, https://doi.org/10.1016/j.iot.2020.100172

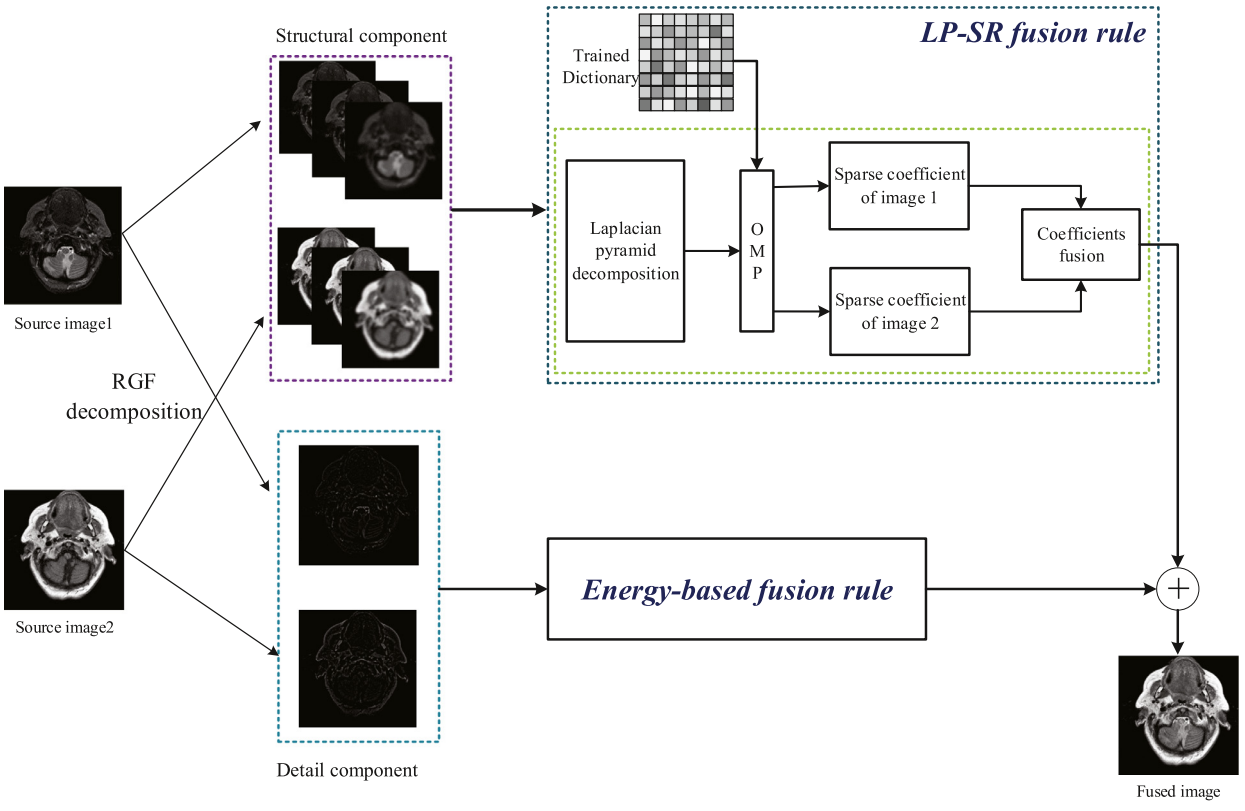

Fig. 1. Synopsis of proposed framework.

3.1. Image decomposition

Applying multi-scale decomposition methods, we can obtain image features at diverse scales. However, the conventional multi-scale decomposition methods adopt linear decomposition mostly, which may cause many artifacts at composite image. Therefore, it is preferred to apply nonlinear multi-scale decomposition in many image processing applications, such as edge-preserving filtering. In this portion, we use edge-preserving filtering, *i.e.* Rolling Guidance Filtering, which can effectively eliminate artifacts, to obtain the best structural components and detail component separated from source image I.

For a source image I, the structural component I_s can be obtained by Eq. 6. N^{iter} is the number of iterations.

$$I_S = RGF(I, \delta_s, \delta_r, N^{iter}). \tag{6}$$

The residuals images of two progressively smooth images, that detail component, can be calculated by Eq. 7

$$I_D = I - I_S. \tag{7}$$

Fig. 2 shows the procedure of decomposition phase with Rolling Guidance Filtering.

3.2. Structural component fusion

For preserving the geometric structure information of source images, the structural component is decomposed into a low-frequency (LF) layer and a sequence of high-frequency (HF) layers via the Laplacian pyramid. We apply different strategies to better preserve effective information in both LF and HF layers. We describe the LF layer by using sparse coefficients with a pre-trained dictionary. Then, we adopt max-L1 rule to decide the optimal sparse coefficients. And the sequence of HF layers can be merged according to max-absolute rule [31]. Fig. 3 shows the structural component fusion framework. The detailed procedures of the phase are as follows:

i) The structural components S_A, S_B are dismantled into LF layer (low_A, low_B) and a sequence of HF layers $\{high_A^i, high_B^i\}_{i=1}^{L}$. L is the numbers of layers.
ii) The LF layer adopts sliding window technique to divide low_A, low_B into image patches from top left to bottom right. The patch size set $\sqrt{n} \times \sqrt{n}$ and a step length set s pixel. Suppose $\{p_A^i\}_{i=1}^{N}$, $\{p_B^i\}_{i=1}^{N}$ denote the image patches in low_A and low_B. N is the number of image patches.

Please cite this article as: J. Chen, L. Zhang and L. Lu et al., A novel medical image fusion method based on Rolling Guidance Filtering, Internet of Things, https://doi.org/10.1016/j.iot.2020.100172

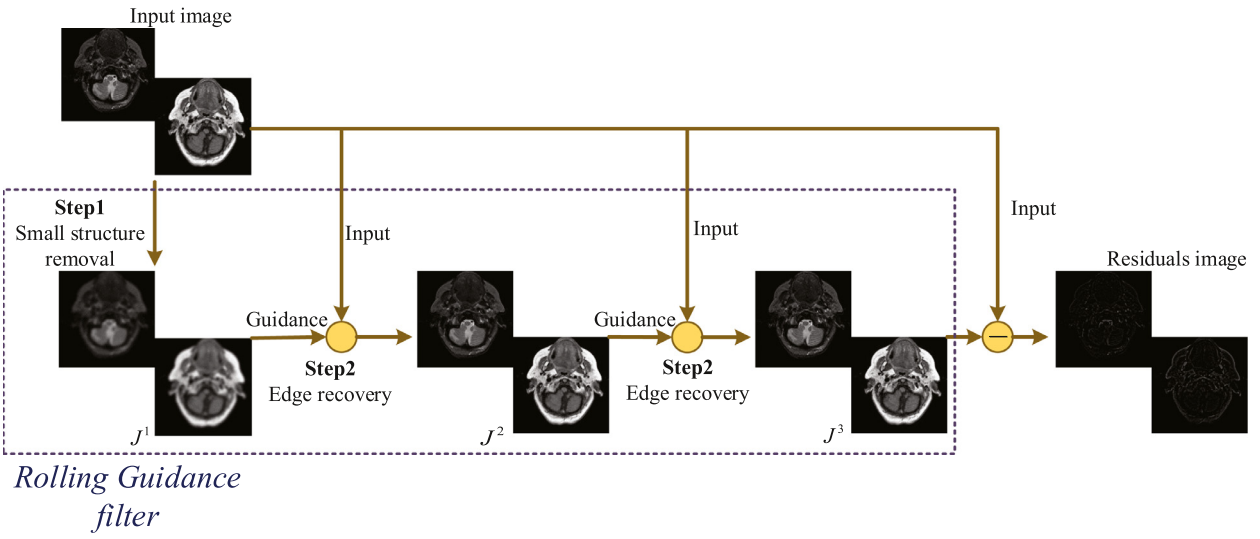

Fig. 2. Flow chart of image decomposition with RGF. The iteration results are got in the third times.

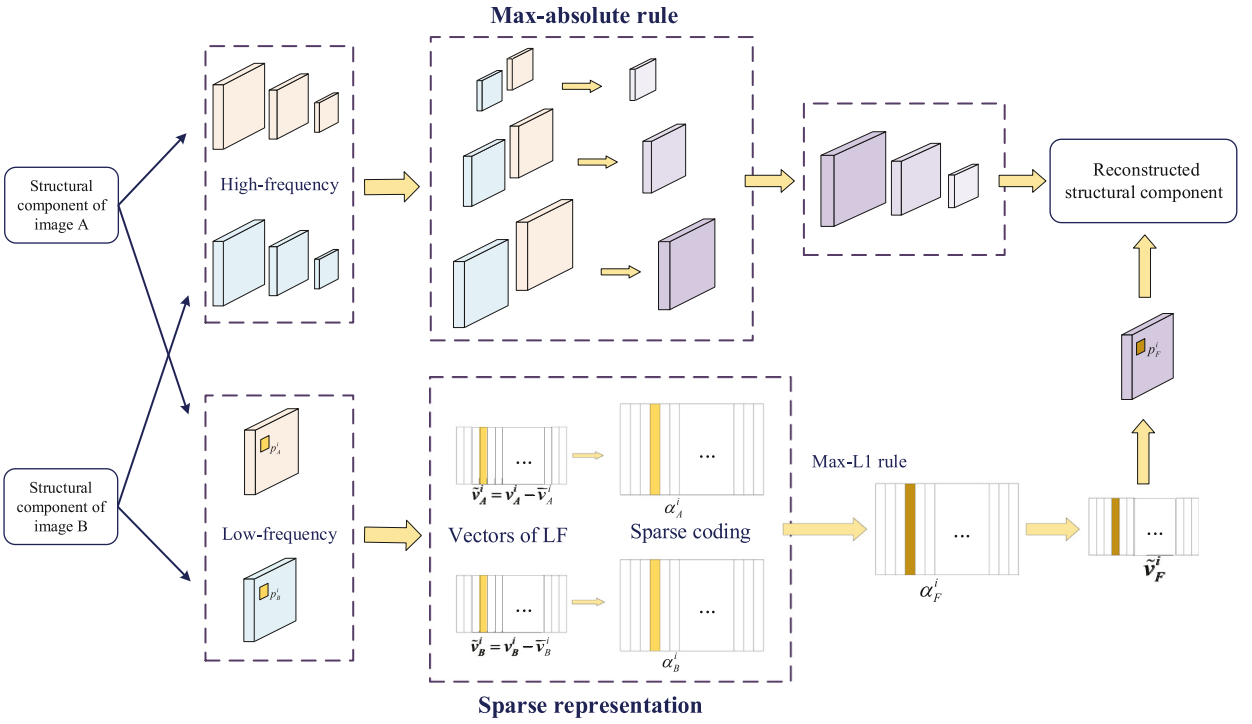

Fig. 3. The diagram of the structural component fusion framework.

iii) Rearrange $\{p_A^i, p_B^i\}_{i=1}^N$ into column vectors $\{v_A^i, v_B^i\}$. $\{\bar{v}_A^i\}, \{\bar{v}_B^i\}$ represents the average values of all the elements in v_A^i and v_B^i, respectively. $\{\tilde{v}_A^i\}, \{\tilde{v}_B^i\}$ can be obtained by

$$\begin{cases} \tilde{v}_A^i = v_A^i - \bar{v}_A^i \cdot \{1\} \\ \tilde{v}_B^i = v_B^i - \bar{v}_B^i \cdot \{1\} \end{cases}, \tag{8}$$

$\{1\}$ is an all-one valued $n \times 1$ vector.

iv) Calculate the sparse coefficient vector (α_A^i, α_B^i) via applying the orthogonal matching pursuit (OMP) algorithm [32] as

$$\begin{cases} \alpha_A^i = \arg\min_{\alpha} \|\alpha\|_0 \quad s.t. \quad \left\|\tilde{v}_A^i - D\alpha\right\|_2 < \varepsilon \\ \alpha_B^i = \arg\min_{\alpha} \|\alpha\|_0 \quad s.t. \quad \left\|\tilde{v}_B^i - D\alpha\right\|_2 < \varepsilon \end{cases}, \tag{9}$$

Please cite this article as: J. Chen, L. Zhang and L. Lu et al., A novel medical image fusion method based on Rolling Guidance Filtering, Internet of Things, https://doi.org/10.1016/j.iot.2020.100172

where D is pre-trained dictionary.

v) The fused sparse vector can be obtained by using the $Max-L1$ rule:

$$\alpha_F^i = \begin{cases} \alpha_A^i & if \quad \left\|\alpha_A^i\right\|_1 > \left\|\alpha_B^i\right\|_1 \\ \alpha_B^i & if \quad \left\|\alpha_A^i\right\|_1 \leq \left\|\alpha_B^i\right\|_1 \end{cases}. \tag{10}$$

The final result can be calculated as

$$v_F^i = D\alpha_F^i + \bar{v}_F^i \cdot \{1\}, \tag{11}$$

where $\bar{v}_F^i$ is $\bar{v}_F^i = \begin{cases} v_A^i & if \quad \alpha_F^i = \alpha_A^i \\ v_B^i & if \quad \alpha_F^i = \alpha_B^i \end{cases}$.

vi) Repeat above processes to get all the fused vectors $\{v_F^i\}_{i=1}^N$. The fused patch $\{p_F^i\}_{i=1}^N$ can be obtained by reshaping v_F^i with size of $\sqrt{n} \times \sqrt{n}$. Let L_F represents the fused result of LF layer, and plug p_F^i into its original position in L_F.

vii) The HF layers $\{high_A^i, high_B^i\}_{i=1}^L$ are fused by applying "max-absolute" rule. Then, a small majority filter is used to implement the consistency verification.

viii) At last, the fused structural component S_F can be reconstructed via inverse Laplacian pyramid.

For one thing, LP can remain the best spectral information and SR has the strengths of adaptive and high-performance representations. For another thing, applying the max-absolute rule to the HF layer preserves the information of the HF layer and increases the speed of calculation.

3.3. Detail component fusion

Sum-modified-Laplacian is especially well-suited to measure the focus of detail image [29]. In this part, we use SML to estimate the energy of the detail component. SML is defined in section 2.3. In this work, we set M, N is 2. We regard P as the energy of image detailed components. P can be defined as $P = \sum_{x,y} \|SML(x,y)\|_1$. $\|\cdot\|_1$ represents the L_1 norm. The rule of detail component fusion can be given by Eq. 12

$$D_F = \sum_{i=1,2,\ldots,k} \frac{P_i}{P_1 + P_2 + \cdots + P_k} D_i, \tag{12}$$

where D_i represents detail component of $i-th$ source image. D_F represents the fused detail component. n is the number of source images.

3.4. Image reconstruction

The final result I_F is derived via fused structural component and detailed component as follow as:

$$I_F = S_F + D_F. \tag{13}$$

4. Experiments and analyses

In this section, we verify the performance of our method by comparing with other methods. Firstly, our experimental setup is given in section 4.1. Then, we analyze the performance evaluation of experiment results in detail in section 4.2.

4.1. Experimental setup

We prepare diverse image pairs for experiments as shown in Fig. 4. The size of test images is 256 × 256. The test image pairs are from http://www.med.harvard.edu/AANLIB/home.html. These parameters setting of the experiment are shown in Table 1. Furthermore, we consider six methods for comparing with our method, *i.e.*, WT [8], CVT [32], NSCT [33], LP [6], GFF [15], SR [26].

We introduce three mainstream metrics of objective evaluation to quantitatively evaluate the performance of diverse methods [34]. These metrics include mutual information (MI), edge retention (Q_{AB}^F), and standard deviation (SD).

MI indicates the information quantifies transferred to the resultant image from the source image. It is estimated by

$$MI_{X,Y}^F = MI(X,F) + MI(Y,F), \tag{14}$$

$$MI(X,Y) = \sum_{x,y} p_{X,Y}(x,y) \log_2 \frac{p_{X,Y}(x,y)}{p_X(x)p_Y(y)}, \tag{15}$$

where $MI(X, Y)$ expresses the mutual information between input images X and Y. $p_X(x)$ and $p_Y(y)$ represent the edge probability distributions function of X and Y. $p_{X,Y}(x, y)$ represents the joint probability distribution function between X and Y.

Please cite this article as: J. Chen, L. Zhang and L. Lu et al., A novel medical image fusion method based on Rolling Guidance Filtering, Internet of Things, https://doi.org/10.1016/j.iot.2020.100172

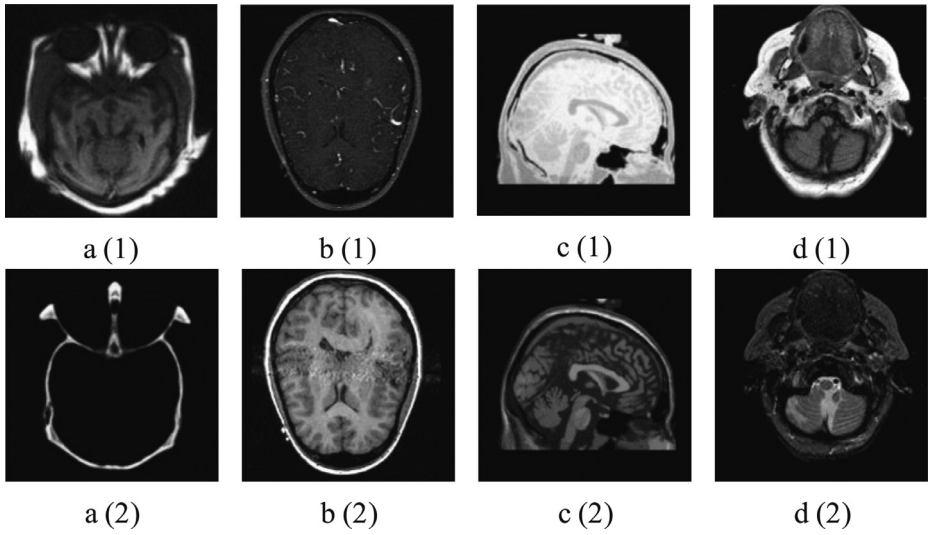

Fig. 4. The diverse image pairs for experiments. a (1) - d (1) are the MRI images. a (2) - d (2) are the CT images, correspondingly.

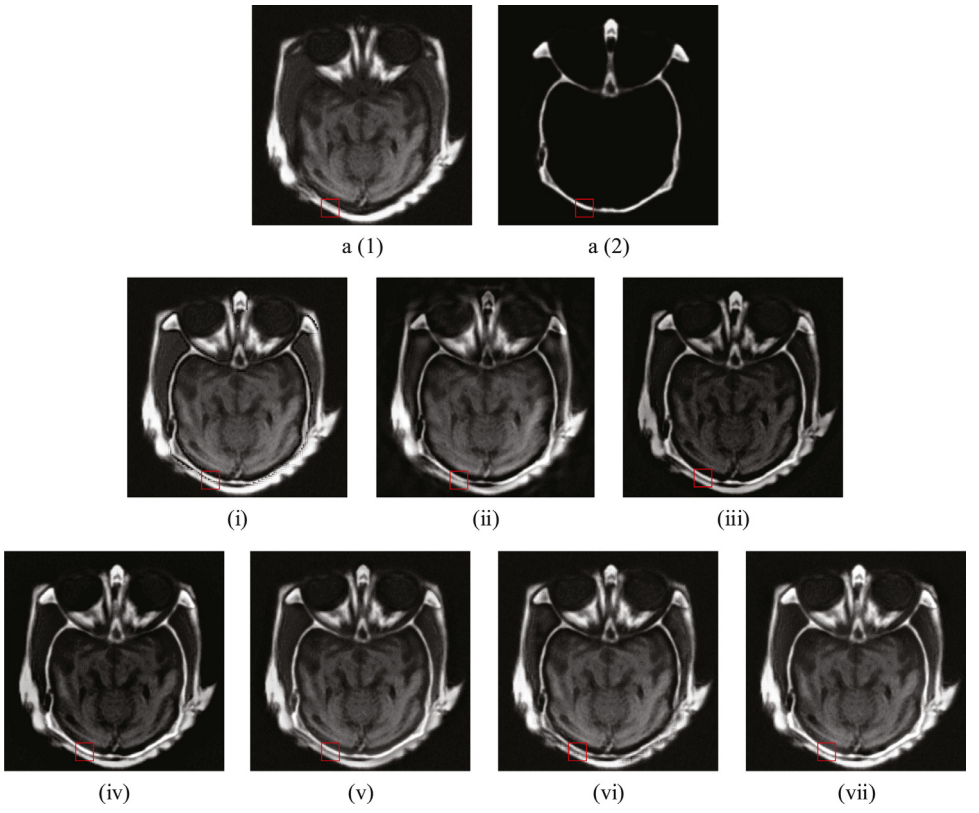

Fig. 5. The fusion images of image 1 by diverse fusion methods. a (1) is MRI image. a (2) is the CT image. (i)-(vii) are the fusion results of the WT, CVT, NSCT, LP, GFF, SR, and the proposed method, separately.

Q_{AB}^{F} is utilized to measure the marginal intensity of fused image contrasted with a source image. Q_{AB}^{F} is defined as

$$Q_{AB}^{F} = \frac{\sum_{x,y} \left(Q^{AF}(x,y)w^{A}(x,y) + Q^{BF}(x,y)w^{B}(x,y)\right)}{\sum_{x,y} \left(w^{A}(x,y) + w^{B}(x,y)\right)}, \tag{16}$$

$$Q^{XY}(x,y) = Q_{g}^{XY}(x,y) + Q_{\alpha}^{XY}(x,y),$$

Please cite this article as: J. Chen, L. Zhang and L. Lu et al., A novel medical image fusion method based on Rolling Guidance Filtering, Internet of Things, https://doi.org/10.1016/j.iot.2020.100172

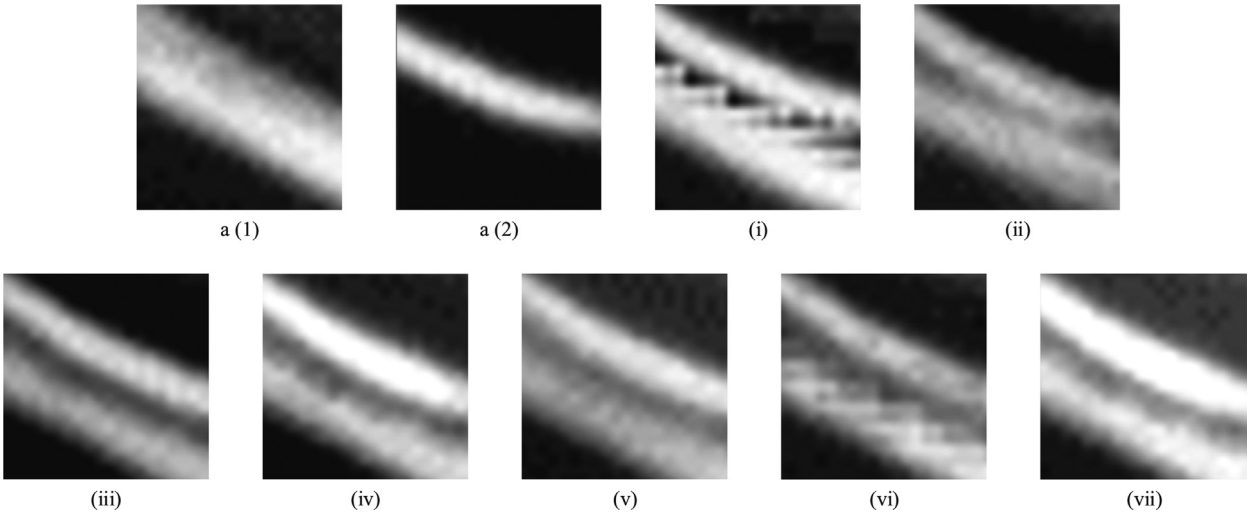

Fig. 6. The magnified version of the red region marked of Fig 5, correspondingly.

Table 1
the parameters setting of experiments

Dictionary learning	atoms = 256 error tolerance = 0.1 iteration times = 32
RGF filtering	level = 1 spatial sigma = 3.0 range sigma = 0.1 iteration times = 3
Laplacian pyramid	level = 5 size = 8 overlap = 1
Sum-modified-Laplacian	size = 3

where $Q_g^{XY}(x, y)$ denotes edge intensity at input image (x, y). $Q_\alpha^{XY}(x, y)$ denotes direction similarity at input images (x, y). $w^*(x, y)$ the weight of $Q^{XY}(x, y)$.

SD can measure the discrete degree of an image. μ is the average value of an image. It is given by

$$SD = \sqrt{\frac{1}{M \times N} \sum_{x=0}^{M-1} \sum_{y=0}^{N-1} [F(x, y) - \mu]^2}. \tag{17}$$

4.2. Subjective and objective evaluation

For subjective comparison, Figs. 5–12 show the subjective effect of fusion results by different methods. The experiment concludes all of these methods can effectively fuse source images. The brightness and contrast of the composite images can be improved by the WT method. However, It is easy to lost information in the fusion process by WT. The CVT, NSCT, LP, and GFF methods can well preserve the information while the brightness and sharpness are undesirable. SR and the proposed method are superior to other methods in information retention. In Fig. 5(i, vi), WT and SR methods produce much redundant information in fused images, such as block effect and artifacts. Fig. 5(ii-iv), the composite images of CVT, NSCT, and LP methods lost some information, such as the left upper at (ii), the left lower at (iii, iv). From Fig. 8, as we can see that our method can better integrate information from MRI and CT images than other methods at some extent. The composite image of WT method has excessive brightness and less information in Fig. 9. The result of SR is chaos and undesirable. The sharpness and brightness of the results by CVT, NSCT, LP, GFF, and SR are unsatisfactory in Fig. 11.

Compared with other methods, the proposed method distinctly reaches a more comfortable brightness and overall contrast. This method can maintain the useful structural information and detail textures of source images but also suppress noise and artifacts at the procedure of fusion.

For the objective evaluation, we exhibit the results of the three metrics in Table 2,3,Table 4. The higher values of MI, Q_{AB}^F, and SD mean the better fusion effects of images are. As shown in Table 2, the value of the proposed method is mostly the best. For image 1, the value of SR is the best, but the subjective result is shown in Fig. 5 has low contrast. And the SR method produce many block effect in the fusion process. Q_{AB}^F is an indicator for evaluating edge retention. We can elicit the

Please cite this article as: J. Chen, L. Zhang and L. Lu et al., A novel medical image fusion method based on Rolling Guidance Filtering, Internet of Things, https://doi.org/10.1016/j.iot.2020.100172

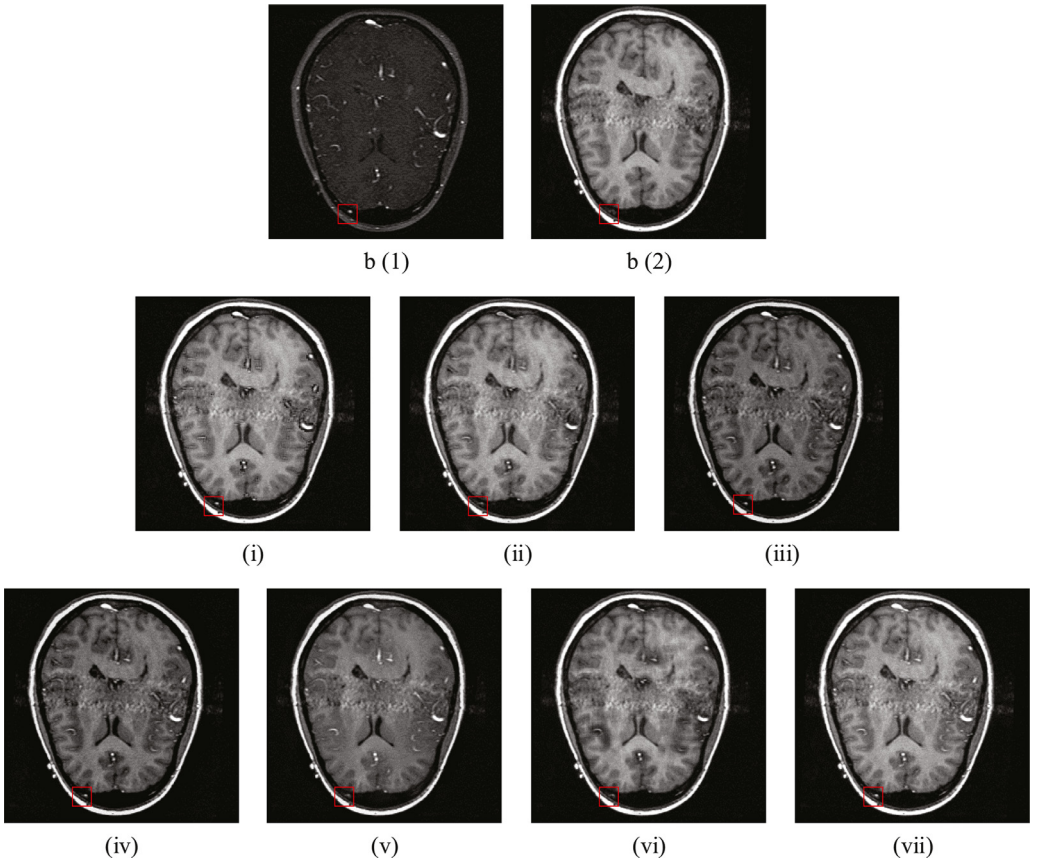

Fig. 7. The fusion images of image 2 by diverse fusion methods. b (1) is MRI image. b (2) is the CT image. (i)-(vii) are the fusion results of the WT, CVT, NSCT, LP, GFF, SR, and the proposed method, separately.

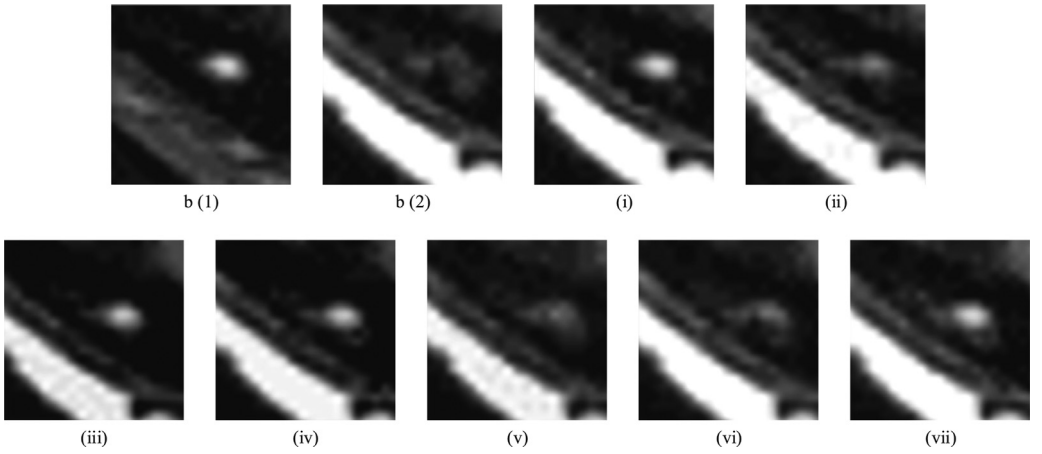

Fig. 8. The magnified version of the red region marked of Fig 7, correspondingly.

Table 2
Quantitative validation with mutual information (MI) of results.

	source images	WT	CVT	NSCT	LP	GFF	SR	Proposed
MI	image 1	2.332	1.956	2.242	2.501	3.459	***4.943***	3.685
	image 2	3.205	4.042	3.428	3.463	3.649	4.655	***4.773***
	image 3	3.078	3.197	3.149	3.188	3.108	3.806	***3.842***
	image 4	3.060	3.878	3.228	3.485	3.458	3.746	***4.697***

Please cite this article as: J. Chen, L. Zhang and L. Lu et al., A novel medical image fusion method based on Rolling Guidance Filtering, Internet of Things, https://doi.org/10.1016/j.iot.2020.100172

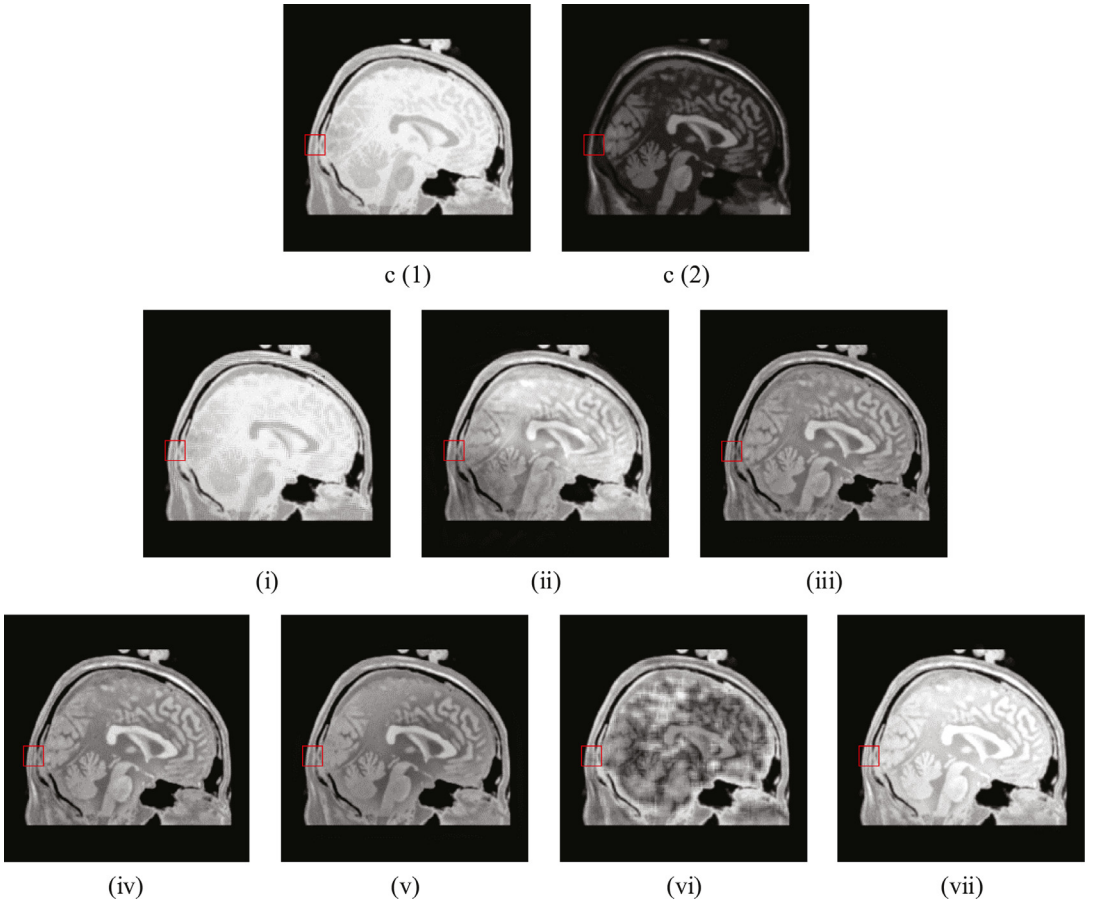

Fig. 9. The fusion images of image 3 by diverse fusion methods. c (1) is MRI image. c (2) is the CT image. (i)-(vii) are the fusion results of the WT, CVT, NSCT, LP, GFF, SR, and the proposed method, separately.

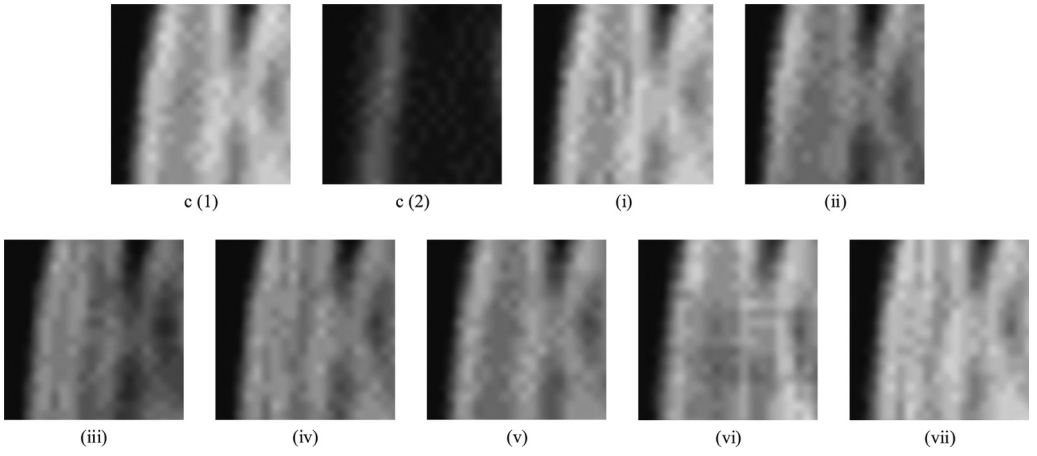

Fig. 10. The magnified version of the red region marked of Fig 9, correspondingly.

Table 3
Quantitative validation with edge retention (Q^F_{AB}) of results.

	source images	WT	CVT	NSCT	LP	GFF	SR	Proposed
Q^F_{AB}	image 1	0.599	0.575	0.705	0.738	***0.775***	0.739	0.767
	image 2	0.525	0.544	0.612	0.619	0.619	0.603	***0.637***
	image 3	0.534	0.589	0.636	0.650	0.656	0.550	***0.664***
	image 4	0.445	0.536	0.560	0.580	0.589	0.489	***0.610***

Please cite this article as: J. Chen, L. Zhang and L. Lu et al., A novel medical image fusion method based on Rolling Guidance Filtering, Internet of Things, https://doi.org/10.1016/j.iot.2020.100172

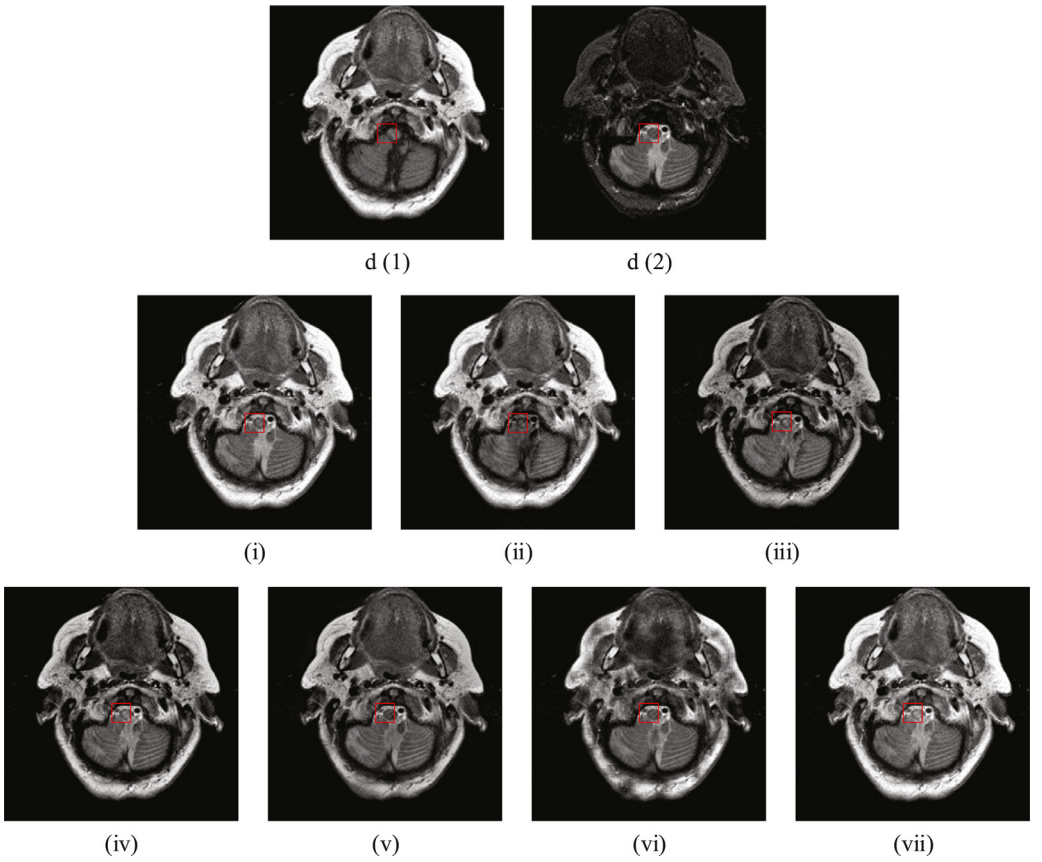

Fig. 11. The fusion images of image 4 by diverse fusion methods. d (1) is MRI image. d (2) is the CT image. (i)-(vii) are the fusion results of the WT, CVT, NSCT, LP, GFF, SR, and the proposed method, separately.

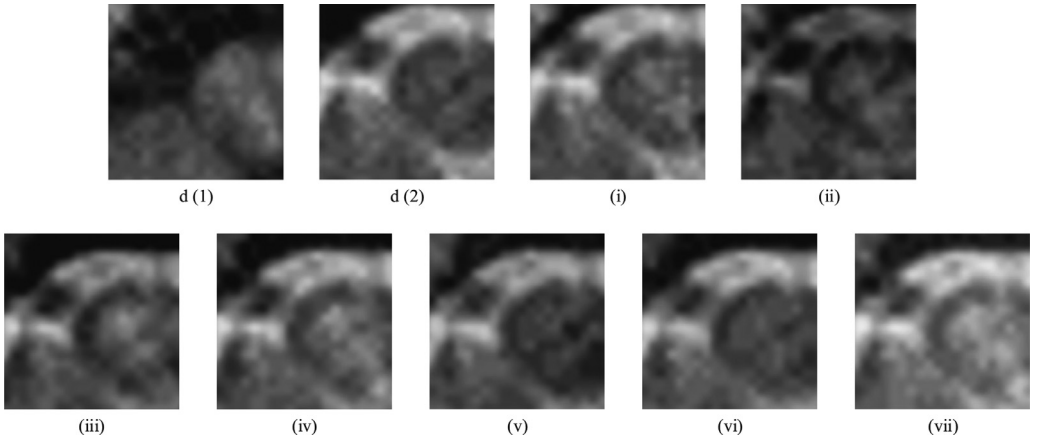

Fig. 12. The magnified version of the red region marked of Fig 11, correspondingly.

Table 4
Quantitative validation with standard deviation (SD) of results.

	source images	WT	CVT	NSCT	LP	GFF	SR	Proposed
SD	image 1	40.479	55.210	46.535	55.233	54.366	55.633	***61.605***
	image 2	51.065	68.589	54.796	57.058	57.953	65.886	***69.287***
	image 3	67.663	87.463	68.806	72.481	67.854	73.803	***101.685***
	image 4	52.503	74.574	56.202	62.521	58.441	60.853	***76.135***

Please cite this article as: J. Chen, L. Zhang and L. Lu et al., A novel medical image fusion method based on Rolling Guidance Filtering, Internet of Things, https://doi.org/10.1016/j.iot.2020.100172

conclusion that our furnish method can effectually fuse valid edge feature from source images. The SD metric denotes the effect of teh overall contrast of an image. From Table 4, the proposed method has the best manifestation of all test image images. As a consequence, the proposed method is excellent for ameliorating the overall contrast.

From the subjective aspect, the proposed method improves the brightness and sharpness of result images, and it is more suited to human visual performance. From the objective aspect, we present method is also significantly more competitive than conventional fusion methods.

5. Conclusion

In this paper, we propose a novel medical image fusion method based on Rolling Guidance Filtering. The method decomposes source images into structural and detail components based on multi-scale decomposition theory. For structural component, the LP-SR based rule is utilized for preserving structure and spectral information. For detail component, a fusion rule of SML is implemented. The scheme based on multi-scale decomposition can effectively extract the interesting information from the source images, whereas the rolling guidance filtering can eliminate artifacts. The proposed fusion scheme achieves the best high-frequency information by take the advantages of multi-scale decomposition and sum-modified-laplacian. In comparison experiments, the average processing time of WT, CVT, NSCT, LP, GFF, SR, and our proposed method are 0.1314 s, 1.6997 s, 2.8379 s, 0.0075 s, 0.5597 s, 14.9052 s, and 0.4304 s, respectively. Therefore our proposed method has the advantage in processing time to acertain extent. In view of the above mentioned, the proposed method is more competitive than traditional method.

Declaration of Competing Interest

No conflict of interest exits in the submission of this manuscript, and manuscript is approved by all authors for publication. I would like to declare on behalf of my coauthors that the work described was original research that has not been published previously, and not under consideration for publication elsewhere, in whole or in part. All the authors listed have approved the manuscript that is enclosed.

Acknowledgment

The authors would like to thank the editors and anonymous reviewers for their insightful comments and constructive suggestions. The research in our paper is sponsored by Open research fund of State Key Laboratory of China (No. 614250304010517).

References

[1] Z. Liu, E. Blasch, V. John, Statistical comparison of image fusion algorithms: Recommendations, Information Fusion (2017) 251–260.
[2] H.A. Eltoukhy, S. Kavusi, A computationally efficient algorithm for multi-focus image reconstruction, in: Proceedings of SPIE - The International Society for Optical Engineering, 5017, 2003, pp. 332–341.
[3] T.M. Tu, S.C. Su, H.C. Shyu, P.S. Huang, A new look at ihs-like image fusion methods, Information Fusion 2 (3) (2001) 177–186.
[4] Z.L. Zhang, S.H. Sun, F.C. Zheng, Image fusion based on median filters and sofm neural networks: : a three-step scheme, Signal Processing 81 (6) (2001) 1325–1330.
[5] K.A. May, M.A. Georgeson, Blurred edges look faint, and faint edges look sharp: The effect of a gradient threshold in a multi-scale edge coding model, Vision Research 47 (13) (2007) 1705–1720.
[6] P.J. Burt, E.H. Adelson, The laplacian pyramid as a compact image code, IEEE Transactions on Communications 31 (4) (2003) 532–540.
[7] A. Toet, Image fusion by a ratio of low-pass pyramid, Pattern Recognition Letters 9 (4) (1989) 245–253.
[8] M. Aharon, M. Elad, A. Bruckstein, K-svd: An algorithm for designing overcomplete dictionaries for sparse representation, IEEE Transactions on signal processin 54 (11) (2006) 4311.
[9] G. Pajares, J.M.D.L. Cruz, A wavelet-based image fusion tutorial, Pattern Recognition 37 (9) (2004) 1855–1872.
[10] J.J. Lewis, R.J. O'Callaghan, S.G. Nikolov, D.R. Bull, C.N. Canagarajah, Pixel- and region-based image fusion with complex wavelets., Information Fusion 8 (2) (2007) 119–130.
[11] Q. Zhang, B.L. Guo, Multifocus image fusion using the nonsubsampled contourlet transform, Signal Processing 89 (7) (2009) 1334–1346.
[12] D. Jiao, W. Li, B. Xiao, Q. Nawaz, Union laplacian pyramid with multiple features for medical image fusion, Neurocomputing 194 (C) (2016) 326–339.
[13] E.J. Candés, D.L. Donoho, Ridgelets: A key to higher-dimensional intermittency? Philosophical Transactions Mathematical Physical & Engineering Sciences 357 (1760) (1999) 2495–2509.
[14] F. Nencini, A. Garzelli, S. Baronti, L. Alparone, in: Remote sensing image fusion using the curvelet transform, 2007, pp. 143–156.
[15] L. Shutao, K. Xudong, H. Jianwen, Image fusion with guided filtering, IEEE Transactions on Image Processing 22 (7) (2013) 2864–2875.
[16] W. Gan, X. Wu, W. Wu, X. Yang, C. Ren, X. He, K. Liu, Infrared and visible image fusion with the use of multi-scale edge-preserving decomposition and guided image filter, Infrared Physics & Technology 72 (2015) 37–51.
[17] J. Wei, X. Yang, W. Wei, L. Kai, A. Ahmad, A.K. Sangaiah, G. Jeon, Medical images fusion by using weighted least squares filter and sparse representation, Computers & Electrical Engineering 67 (x) (2018) 252–266.
[18] Z. Qi, X. Shen, X. Li, J. Jia, Rolling guidance filter, 2014.
[19] L. Shuaiqi, Z. Jie, S. Mingzhu, Medical image fusion based on rolling guidance filter and spiking cortical model, Computational and Mathematical Methods in Medicine,2015,(2015-6-3) 2015 (2015) (2015) 156043.
[20] L. Jian, Multi-scale image fusion through rolling guidance filter, Future Generation Computer Systems (2018). S0167739X17317892
[21] S. Li, H. Yin, L. Fang, Remote sensing image fusion via sparse representations over learned dictionaries, IEEE Transactions on Geoscience & Remote Sensing 51 (9) (2013) 4779–4789.
[22] R. Chellappa, Sparse Representations and Compressive Sensing for Imaging and Vision, 2013.
[23] J. Zhang, D. Zhao, F. Jiang, W. Gao, Structural group sparse representation for image compressive sensing recovery, 2013.
[24] M. Nejati, S. Samavi, S. Shirani, Multi-focus image fusion using dictionary-based sparse representation, Information Fusion 25 (2015) 72–84.

Please cite this article as: J. Chen, L. Zhang and L. Lu et al., A novel medical image fusion method based on Rolling Guidance Filtering, Internet of Things, https://doi.org/10.1016/j.iot.2020.100172

[25] H. Yin, Y. Li, C. Yi, Z. Liu, Z. Zhu, A novel sparse-representation-based multi-focus image fusion approach, Neurocomputing 216 (C) (2016). S0925231216307950
[26] B. Yang, S. Li, Multifocus image fusion and restoration with sparse representation, IEEE Transactions on Instrumentation & Measurement 59 (4) (2010) 884–892.
[27] Q. Li, X. Yang, W. Wu, K. Liu, G. Jeon, Multi-focus image fusion method for vision sensor systems via dictionary learning with guided filter, Sensors 18 (7) (2018) 2143.
[28] Q.Z. Zhi, H. Yin, C. Yi, Y. Li, G. Qi, Q.Z. Zhi, H. Yin, C. Yi, Y. Li, G. Qi, A novel multi-modality image fusion method based on image decomposition and sparse representation, Information Sciences (2017).
[29] S.K. Nayar, Y. Nakagawa, Shape from focus, IEEE Transactions on Pattern Analysis & Machine Intelligence 16 (8) (1989) 824–831.
[30] Z. Zhu, Y. Chai, H. Yin, Y. Li, Z. Liu, A novel dictionary learning approach for multi-modality medical image fusion, Neurocomputing 214 (2016) 471–482.
[31] L. Yu, S. Liu, Z. Wang, A general framework for image fusion based on multi-scale transform and sparse representation, 2015.
[32] S.G. Mallat, Z. Zhang, Matching pursuits with time-frequency dictionaries, IEEE Trans on Signal Processing 41 (12) (1993) 3397–3415.
[33] G. Piella, A general framework for multiresolution image fusion: from pixels to regions, Information Fusion 4 (4) (2003) 259–280.
[34] X.L. Zhang, L.I. Xiong-Fei, L.I. Jun, Validation and correlation analysis of metrics for evaluating performance of image fusion, Acta Automatica Sinica 40 (2) (2014) 306–315.

Please cite this article as: J. Chen, L. Zhang and L. Lu et al., A novel medical image fusion method based on Rolling Guidance Filtering, Internet of Things, https://doi.org/10.1016/j.iot.2020.100172